Earth and Planetary Science Letters, 100 (1990) 210–225
Elsevier Science Publishers B.V., Amsterdam

[CL]

Enriched back-arc basin basalts from the northern Mariana Trough: implications for the magmatic evolution of back-arc basins

Robert J. Stern [a], Ping-Nan Lin [a,1], Julie D. Morris [b], Michael C. Jackson [c], Patricia Fryer [c], Sherman H. Bloomer [d] and Emi Ito [e]

[a] *Center for Lithospheric Studies, University of Texas at Dallas, Richardson, TX 75083-0688, U.S.A.*
[b] *Department of Terrestrial Magnetism, Carnegie Institution of Washington, 5241 Broad Branch Rd., NW, Washington, DC 20015, U.S.A.*
[c] *Hawaii Institute of Geophysics, University of Hawaii, 2525 Correa Rd., 0228tHonolulu, HI 96822, U.S.A.*
[d] *Department of Geology, Boston University, 675 Commonwealth Ave., Boston, MA 02215, U.S.A.*
[e] *Department of Geology and Geophysics, University of Minnesota, 310 Pillsbury Dr., SE, Minneapolis, MN 02215, U.S.A.*

Accepted for publication March 20, 1990

ABSTRACT

The composition of basalts erupted at the earliest stages in the evolution of a back-arc basin permit unique insights into the composition and structure of the sub-arc mantle. We report major and trace element chemical data and O-, Sr-, Nd-, and Pb-isotopic analyses for basalts recovered from four dredge hauls and one ALVIN dive in the northern Mariana Trough near 22° N. The petrography and major element chemistry of these basalts (MTB-22) are similar to tholeiites from the widest part of the Trough, near 18° N (MTB-18), except that MTB-22 have slightly more K_2O and slightly less TiO_2. The trace element data exhibit a very strong arc signature in MTB-22, including elevated K, Rb, Sr, Ba, and LREE contents; relatively low K/Ba and high Ba/La and Sr/Nd. The Sr- and Nd- isotopic data plot in a field displaced from that of MTB-18 towards Mariana arc lavas, and the Pb-isotopic composition of MTB-22 is indistinguishable from Mariana arc lavas and much more homogeneous than MTB-18. Mixing of 50–90% Mariana arc component with a MORB component is hypothesized. We cannot determine whether this resulted from physical mixing of arc mantle and MORB mantle, or whether the arc component is introduced by metasomatism of MORB-like mantle by fluids released from the subducted lithosphere. The strong arc signature in back-arc melts from the Mariana Trough at 22° N, where the back-arc basin is narrow, supports general models for back-arc basin evolution whereby early back-arc basin basalts have a strong arc component which diminishes in importance relative to MORB as the back-arc basin widens.

1. Introduction

The relationship of the magma source of back-arc basins to that of island arcs is an important and unresolved problem. Of particular petrologic interest is how arc and back-arc basin (BAB) magma sources evolve with time, because a better understanding of this should lead to firmer constraints on the distribution and melting history of these mantle sources. For mature systems, the magma sources are isotopically distinguishable and the interplay between sources and melting regimes leads to distinctly different major and trace element characteristics for arc and BAB melts. Arc magmas are characterized by large ion lithophile element (LILE) enrichments and high-field strength cation (HFSC) depletions and have more radiogenic Sr and less radiogenic Nd while BAB melts are very similar to mid-ocean ridge basalt (MORB), with minor or no LILE enrichment and no HFSC depletions. For mature systems, the geographic separation between the volcanic front of the arc and the BAB rift readily allows for distinct magma sources, mantle flow lines, and thermal regimes to be maintained. In contrast, initial back-arc rifts develop within or very close to the arc [1,2]; this requires that arc and initial BAB sources either be identical or closely juxtaposed within the upper 150 km of the sub-arc

[1] Present address: Byrd Polar Research Center, Ohio State University, 125 S. Oval Mall, Columbus, OH 43210, U.S.A.

0012-821X/90/$03.50

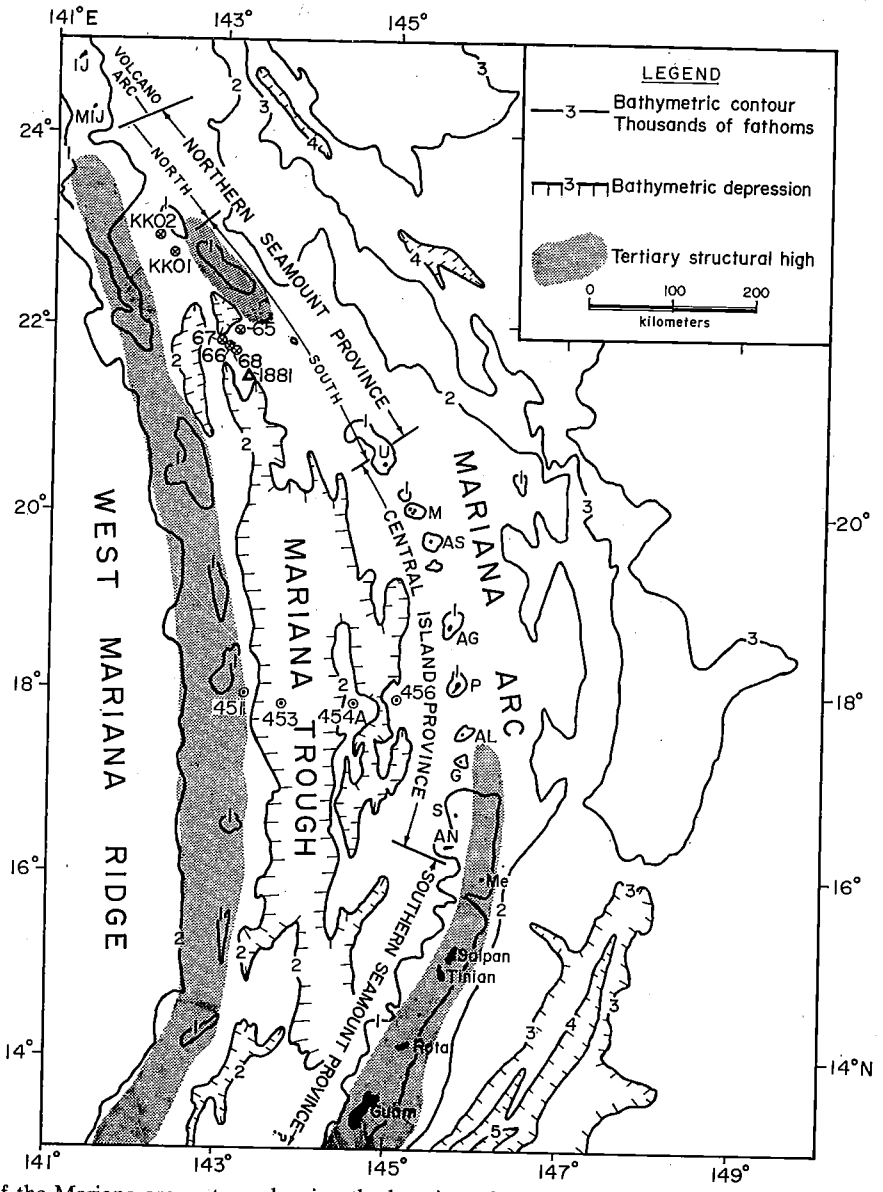

Fig. 1. Locality map of the Mariana arc system, showing the location of sampling sites discussed in this study. Also shown are the location of DSDP Leg 60 drill sites, sited along 18° N and KK-1 and KK-2 dredge sites, farther to the north in the Mariana Trough.

mantle. The magmatic evolution of a back-arc basin can be expected to show how fast the BAB source comes to lose its arc-like character, and this information leads to new insights about mantle convection at convergent margins, the dimensions of the mantle wedge affected by slab-derived fluids, and the distribution of sources in the mantle wedge.

The purpose of this paper is to contribute to our understanding of back-arc basin evolution by reporting the results of geochemical and isotopic studies of samples recovered in the northernmost Mariana Trough. The Mariana Trough, one of the best-documented examples of an active back-arc basin, has been the focus of abundant geophysical, DSDP, and dredging studies [e.g., 3–7]. There exists an extensive database of geochemical and isotopic studies of Mariana Trough basalts (MTB) [8–14,16,30,49,50] but these are primarily clustered around 18° N, where the Mariana Trough is widest and, probably, most mature (Fig. 1). Samples for this study come from the northernmost part of the Mariana Trough, just south of 22° N; for the sake of brevity we refer to these as MTB-22 and compare them throughout this study with MTB-18.

It has been argued that the northward narrowing of the Mariana Trough reflects the northward

propagation of rifting [14]. In this case, MTB-22 correspond to early BAB melts. It has also been suggested that the northward termination of the Mariana Trough is a consequence of slower spreading due to the collision of the Ogasawara Plateau with the trench at 26°N [15]. In either case, MTB-22 correspond to mantle melts generated close to arc sources. Comparison of geochemical and isotopic data for MTB-22 with MTB-18 and with the Mariana arc itself promises to provide new constraints on the relationship between arc and BAB mantle sources and melting regimes.

2. Sample locations and petrography

The samples come from four dredges of the 1985 cruise of the R/V *T.G. Thompson* (TT-192, D-65 to 68) and one ALVIN dive in 1987(1881; approximate locations are shown in Fig. 1). Dredges 66, 67, and 68 were from the SE end of a NW–SE trending high centered on 21°55′N, 143°E that probably marks the present spreading axis (D-66: 21°47′N, 143°06′E, 3575–3920; D-67: 21°50′N, 143°03′E, 3290–3710 m; D-68: 21°42′N, 143°10′E, 3100–3385 m). ALVIN dive 1881 (21°35′N, 143°16′E, 3100–3300 m) is from farther SE along this trend, in a region where a maximum of fresh basaltic flows were observed from ALVIN; correspondence between the bathymetric evidence and seafloor observations of abundant fresh basalt flows indicates that all of the above samples are from an actively spreading ridge segment. Dredge 65 is from the southern flank of a 400 m high seamount (21°54′N, 143°05′E, 2530–3150 m), about 10 km NE of the spreading axis sampled at D-67.

All of the samples analyzed here are aphyric to porphyritic or vitrophyric, with phenocrysts of plagioclase, clinopyroxene, and less commonly, olivine; all lavas have abundant vesicles (Appendix 1). Dredge 66 had some Mn-coated basalts and some altered basalts were recovered on D67. Care was taken to obtain petrographically fresh specimens of all sample sites for geochemical and isotopic analyses.

3. Analytical techniques

Major elements were analyzed by a combination of XRF and atomic absorption analyses of rock powders and electron microprobe (HIG Cameca MBX) analyses of natural glasses; analytical details are reported elsewhere [16]. Trace elements were analyzed by isotope dilution at UTD, except for Pb, analyzed at DTM; procedures, total processing blanks, and standard values are discussed elsewhere [17]. Sr and Nd isotopic compositions were determined using a MAT 261 multi-collector solid-source mass spectrometer at UTD. Sr was isolated using standard cation-ex-

TABLE 1
Major elements analyses, MTB-22

	65201		6503		6504	6605		6606		6705	6707
	1	2	1	2	1	1	2	1	2	1	1
SiO_2	53.98	54.42	54.89	54.86	53.90	49.05	50.61	48.67	51.09	51.75	51.14
TiO_2	1.13	1.10	1.11	1.22	1.11	0.80	0.91	0.79	0.92	1.01	1.41
Al_2O_3	15.99	16.03	16.58	15.52	16.36	16.02	16.33	15.71	16.36	16.76	15.54
$Fe_2O_3^T$	9.87	9.73	9.67	10.16	9.71	8.53	8.73	8.45	9.42	9.17	10.90
MnO	ND	ND	0.17	ND	ND	ND	ND	ND	ND	ND	ND
MgO	4.59	4.61	4.78	4.25	4.78	10.07	7.12	9.82	6.63	6.24	4.80
CaO	8.76	8.37	8.92	8.44	9.01	12.23	12.43	12.09	11.74	11.21	9.23
Na_2O	3.32	3.39	3.59	3.40	3.27	2.04	2.36	2.21	2.49	2.75	3.01
K_2O	0.65	0.35	0.60	0.40	0.56	0.28	0.32	0.30	0.33	0.57	0.49
P_2O_5	0.13	ND	0.13	ND	0.14	0.08	ND	0.08	ND	0.16	0.16
TOTAL	98.42	98.00	100.44	98.25	98.84	99.10	98.81	98.12	98.96	99.62	96.68
$Mg^{\#}$	56	56	57	53	57	76	69	76	65	65	54
CaO/Al_2O_3	0.55	0.52	0.54	0.54	0.55	0.76	0.76	0.77	0.72	0.67	0.59

1 = XRF whole rock [16]; 2 = Glass, Electron Microprobe [16]; $Mg^{\#} = 100[Mg/Mg + Fe^{2+}]$; FeO/Fe_2O_3 adjusted using the method of [56] i.e., $Fe_2O_3 = TiO_2 + 1.5$.

change techniques, with a total processing blank of 2 ng. Both unleached and leached samples were analyzed for Sr; leaching was accomplished by placing powders in 2.5*N* HCl for 12 h. Sr was analyzed in the static mode and fractionation-corrected to $^{86}Sr/^{88}Sr = 0.1194$; 31 analyses of E&A $SrCO_3$ yielded a mean $^{87}Sr/^{86}Sr$ of 0.70806 ± 3 (total range) and $^{84}Sr/^{86}Sr$ of 0.056488 ± 40 (total range). Nd was isolated using a procedure modified after Richard et al. [18]; total processing blanks for Nd are about 0.5 ng. Analyses were done in the multicollection dynamic mode and fractionation-corrected to $^{146}Nd/^{144}Nd = 0.7219$; 23 analyses of the UCSD Nd standard yielded a mean $^{143}Nd/^{144}Nd$ of 0.511848 ± 10 (total range) and a mean $^{145}Nd/^{144}Nd$ of 0.3484011 ± 8 (total range). The BCR-1 standard has a $^{143}Nd/^{144}Nd$ of 0.51262, and we take this as equal to the isotopic composition of the bulk earth for the purpose of calculating epsilon-Nd. Lead isotopes were analyzed at DTM on the VG 354 multicollector mass spectrometer in the static mode following well-established procedures [19]; Pb isotope ratios are reproducible and accurate to 0.05% per amu.

All samples were analyzed for a $\delta^{18}O$; oxygen was extracted using ClF_3 [20], similar to the BrF_5 method [21]. The resulting CO_2 gas was analyzed with a Finnigan MAT Delta E triple-collector 90° sector mass spectrometer. Oxygen isotope ratios were normalized against SLAP ($\delta^{18}O_{VSMOW} = -55.0$). The $\delta^{18}O$ for NBS-28 Quartz using this technique is $+9.50 \pm 0.15$, also relative to VSMOW. The reproducibility of whole-rock samples is better than ± 0.3. Because of subtle alteration effects on the whole rock samples and because we want to characterize the magmatic compositions, we only report the three samples of glass in Table 3.

4. Results

Major element data for the twelve samples are listed in Table 1, in most cases with XRF whole rock (WR) and electron microprobe glass data for the same sample. All are basalts and basaltic andesites. The basalts ($SiO_2 < 52\%$) are approximately saturated in silica, being either olivine normative or only slightly quartz-normative; all are tholeiites. All samples have moderate potassium contents, from 0.28 to 0.61% K_2O for WR and 0.32 to 0.59% for glasses. In most cases—and as expected for aphyric to porphyritic basalts—concentrations of incompatible elements TiO_2, Na_2O, and K_2O in the glass are closely comparable to those in the WR. This observation is especially important in the case of TiO_2, because it indicates that Ti-bearing minerals are not important liquidus phases. Comparison of K_2O contents between D65 WR and glass samples indicates that the WR contains more K_2O than the glass. This suggests that alteration may have ad-

6708		6801		6803		1881-4		1881-7	
1	2	1	2	1	2	1	2	1	2
49.08	51.84	49.03	51.97	48.88	51.66	52.35	53.01	53.95	54.48
0.92	1.07	0.98	1.15	0.90	1.04	1.01	1.13	1.32	1.51
15.08	16.65	15.77	16.54	15.58	16.53	17.30	16.33	16.81	15.57
9.03	7.99	7.89	8.16	8.26	7.83	8.52	9.08	9.41	10.23
ND	ND	ND	ND	ND	ND	0.15	0.13	0.16	0.15
10.73	6.37	9.25	6.31	9.59	6.60	6.50	6.05	5.12	4.31
10.41	11.57	10.79	11.22	10.34	11.42	11.01	10.56	9.17	8.52
2.27	2.73	2.55	2.76	2.49	2.63	2.86	2.89	3.44	3.57
0.45	0.38	0.59	0.59	0.52	0.55	0.46	0.41	0.61	0.49
0.13	ND	0.16	ND	0.16	ND	0.13	0.19	0.18	0.22
98.10	98.60	97.01	98.70	96.72	98.26	100.29	99.78	100.17	99.05
76	70	77	69	76	71	68	65	61	54
0.69	0.69	0.68	0.68	0.66	0.69	0.64	0.65	0.55	0.55

ded a significant amount of K_2O. This is surprising because WR Na_2O contents are nevertheless lower than that of the corresponding glass. The similarity of WR-glass chemistry together with the pristine appearance of the phenocrysts and $^{87}Sr/^{86}Sr$ ratios being largely unaffected by leaching (reported below) indicates that alteration generally has been slight. Alteration for D65 samples is the most extensive of the suite reported here, and even for these we believe that alteration has been slight enough that the Pb, Ba and REE contents and Nd- and Pb- isotopic compositions were unaffected. For the other samples, the correspondence between our petrographic observations, glass-WR comparisons, invariance of $^{87}Sr/^{86}Sr$ determined before and after leaching, and WR $\delta^{18}O$ (+5.7 to +6.5) indicates that these are fresh, and that the trace element and isotopic values are magmatic.

The Mg# of MTB-22 shows a wide range [WR Mg# = 54–77 (mean = 67); glass Mg# = 53–71 (mean = 64)] and indicates extents of fractionation that are similar to MTB-18 (mean Mg# = 63 ± 4 (errors on means are hereafter reported as 1 std. dev.); [8,9,11–13]); these are generally less fractionated than basalts and basaltic andesites from the Mariana arc, (Mg# = 54 ± 8) [12,22–25]. In contrast, the TiO_2 contents of MTB-22 (WR = 1.01% ± 0.16%; glass = 1.12% ± 0.18%) are intermediate between those of the Mariana arc (0.85% ± 0.20%; [12,13,22–25,27–29]) and MTB-18 (1.21% ± 0.26%; [8,9,11–13,26]). A plot of TiO_2 vs. MgO (Fig. 2) shows that for samples with 4–8% MgO, MTB-22 have less TiO_2 than MTB-18. This suggests that the lower TiO_2 of MTB-22 may be a source effect.

Trace element data for MTB-22 are listed in Table 2. Compared with MTB-18, MTB-22 are enriched in LIL and LREE. There is a marked enrichment in Rb, K, Sr, and Ba from south to north in the Mariana Trough, and a corresponding decrease in K/Ba and increase in Sr/Nd and Ba/Sr in the same direction (Fig. 3); no systematic variation in K/Rb is observed. Note that the trends indicate an overall pattern of increasing arc-like signature from south to north (although rare MTB-18 have arc-like trace element characteristics [12,30]). For example, MTB-22 has a mean K/Ba of 37 ± 10, significantly lower than N-MORB (~ 64) [31] and MTB-18 (74 ± 35) [8,9,14]. It is also useful to compare this and other ratios between MTB-18 and MTB-22 and the adjacent parts of the Mariana arc. For example, the mean K/Ba of Central Island Province (CIP) which flanks MTB-18 is 31 ± 9 while that of the southern portion of the Northern Seamount Province (S-NSP), lying next to MTB-22, is 23 ± 4 (Fig. 1) [17]. K/Ba for MTB-22 is thus more similar to that of the arc than either N-MORB or MTB-18. Similarly, mean Sr/Nd for MTB-22 is 25 ± 3, higher than N-MORB (~ 10) [31] or MTB-18 (19 ± 5) [8,9,14,30] and approaching that of the Mariana arc CIP (34 ± 11) and S-NSP (30 ± 11) [17]. Ba/La for MTB-22 is 17 ± 4, much higher than values for N-MORB of about 3.6 [31] and MTB-18 of 7.5 ± 5 [12] and approaching the mean Ba/La of 37 ± 13 and 35 ± 15, respectively, for the CIP and S-NSP of the Mariana arc [17]. The latitudinal variation appears to principally manifest enrichment of alkaline earths—and especially Ba—relative to the alkali metals and to the REE. The marked enrichment of Ba is a diagnostic feature of arc magmas [32] and is especially apparent for MTB-22 from latitudinal plots of Sr/Nd and Ba/Sr (Fig. 3).

The REE patterns for MTB-18 and MTB-22 also indicate enrichments of incompatible elements to the north. MTB-18 have nearly flat or slightly LREE-enriched REE patterns, with no significant enrichment of Ba relative to the LREE (Fig. 4). In contrast, MTB-22 are enriched in LREE and depleted in HREE (mean $(La/Yb)_n$ = 2.0 ± 0.4) and are enriched in Ba relative to LREE. MTB-22 also have a small but invariably positive Eu anomaly (Eu/Eu* = 1.06 ± 0.03). All MTB-22 have negative Ce anomalies (Fig. 5), with mean Ce/Ce* = 0.89 ± 0.04. This is remarkably similar to both the Mariana arc CIP and S-NSP, although the determination of Ce/Ce* for REE patterns such as those of MTB-22 (i.e., rapid increase over the LREE) is more uncertain than for more nearly flat or LREE-depleted patterns. Negative cerium anomalies are argued to be characteristic of some arcs, including the Mariana arc [33,34]; MTB-18 REE patterns do not include La, Ce, and Nd so Ce anomalies for these rocks cannot be evaluated.

Contents of Pb in MTB-22 are higher than typical for MTB-18; MTB-22 contains 1.5 ± 0.2 ppm Pb, compared to 0.74 ± 0.25 ppm for nine samples of MTB-18 [30,35]. Pb/Ce ratios average 0.10 ± 0.02, much higher than the upper mantle

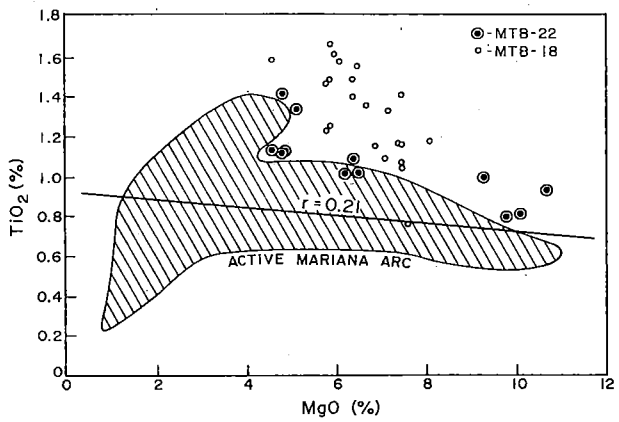

Fig. 2. Plot of MgO vs. TiO_2 for MTB-22, MTB-18 [8,9,11,12,26,54], and active Mariana arc [22–25,27–29,33]. Note that MTB-22, at a given MgO content, is intermediate in TiO_2 between MTB-18 and active Mariana arc lavas. Correlation coefficient r is for Mariana arc samples.

value of 0.036 [36]. Linear extrapolation of Ce concentration from Sm and Nd contents of seven samples of MTB-18 also analyzed for Pb concentration [30] suggests Pb/Ce of 0.048 ± 0.011. Pb/Ce for MTB-22 approaches that of 0.22 ± 0.09 for Fukujin in the Mariana arc S-NSP [12], the only Mariana arc volcano which has such data.

Sr-, Nd-, Pb- and O-isotopic compositions are listed in Table 3. For the most part, $^{87}Sr/^{86}Sr$ of MTB-22 showed little variation between leached and unleached samples. The $^{87}Sr/^{86}Sr$ for D65 samples decreased by 0.0001 following leaching, a result that is consistent with the inference of slight alteration based on K_2O contents of glass and WR. All other samples showed no analytically discernible change. We therefore accept the range observed for the leached samples (0.70309–0.70352) as representing $^{87}Sr/^{86}Sr$ of MTB-22 magmas, with the exception of D65 samples. For these, the $^{87}Sr/^{86}Sr$ of leached samples is only a maximum; magmatic values could have been lower.

The $^{87}Sr/^{86}Sr$ for leached MTB-22 is generally higher than that of MTB-18 (0.70264–0.70333 (Fig. 6a), and overlaps the $^{87}Sr/^{86}Sr$ of the Mariana arc CIP (mean = 0.70342 [37]). It is noteworthy that

TABLE 2
Trace element data

	Dredge 65			Dredge 66		Dredge 67			Dredge 68		ALVIN-1881	
	65201	6503	6504	6605	6606	6705	6707	6708	6801	6803	4	7
K(ppm)	4740	4810	4410	2240	2320	4580	4030	3640	4690	4250	3590	4930
Rb	6.8	7.6	6.8	4.5	4.4	9.3	6.2	6.7	9.2	7.6	6.5	7.5
Sr	236	256	233	238	239	295	272	206	318	275	272	249
Ba	120	120	118	120	122	110	134	84.6	101	94	104	105
La	6.84	5.83	6.07	5.51	5.28	8.91	7.02	5.62	8.46	7.75	6.99	9.50
Ce	13.8	13.7	13.6	12.1	11.3	19.4	16.9	13.4	17.4	16.9	15.3	18.3
Nd	9.84	10.1	10.0	8.41	8.09	12.6	13.0	9.44	11.5	10.6	10.1	12.5
Sm	2.94	2.94	2.90	2.31	2.30	3.41	3.91	2.58	3.11	2.85	2.82	3.50
Eu	1.12	1.16	1.16	0.89	0.90	1.21	1.43	0.96	1.18	1.09	1.06	1.28
Gd	3.54	3.66	3.61	2.83	2.86	4.03	4.55	3.19	3.53	3.37	3.18	4.17
Dy	4.24	4.18	4.16	3.12	3.14	4.24	5.43	3.51	3.91	3.55	3.66	4.61
Er	2.57	2.66	2.55	1.86	1.86	2.58	3.42	2.11	2.34	2.18	2.18	2.86
Yb	2.55	2.64	2.57	1.78	1.78	2.41	3.34	2.07	2.29	2.07	2.18	2.86
Pb	1.42	1.84	1.77	–	1.53	1.59	1.92	1.20	1.38	1.31	1.39	1.52
Elemental ratios												
K/Rb	697	633	649	498	527	492	650	543	510	560	552	657
K/Ba	39.5	40.2	37.4	18.6	18.6	41.6	30.1	43	46.4	45.2	34.4	47.1
Ba/La	17.5	20.6	19.4	21.8	23.1	12.3	19.1	15.1	11.9	12.1	14.9	11.1
Sr/Nd	24.0	25.4	23.3	28.3	28.3	23.5	21.0	21.8	27.6	26.0	27.0	19.9
Ce/Ce*[1]	0.83	0.92	0.89	0.89	0.87	0.90	0.92	0.94	0.86	0.92	0.90	0.81
Eu/Eu*[2]	1.07	1.09	1.10	1.07	1.07	1.00	1.04	1.03	1.09	1.08	1.08	1.03
$(La/Yb)N^3$	1.8	1.5	1.6	2.1	2.1	2.5	1.4	1.8	2.5	2.5	2.1	2.2
Pb/Ce	0.10	0.13	0.13	–	0.14	0.082	0.11	0.09	0.079	0.078	0.091	0.083

[1] Ratio of Ce determined interpolated from La and Nd contents.
[2] Ratio of Eu determined to that interpolated from Sm and Gd contents.
[3] Ghondrite-normalized ratio of La to Yb.

TABLE 3
Isotopic data

Sample	$^{87}Sr/^{86}Sr$ [a]		$^{143}Nd/^{144}Nd$	ϵ_{Nd}	$^{206}Pb/^{204}Pb$ [b]	$^{207}Pb/^{204}Pb$ [b]	$^{208}Pb/^{204}Pb$ [b]	$\delta^{18}O$
	Unleached	Leached						
65201	0.70319+/−3	0.70309+/−3	0.513036+/−13	+8.1	18.734	15.570	38.532	–
6503	0.70323+/−3	0.70314+/−3	0.513007+/−10	+7.5	18.727	15.561	38.497	+6.1
6504	0.70321+/−3	0.70311+/−3	0.512980+/−10	+7.0	18.777	15.572	38.544	–
6605	0.70347+/−3	0.70348+/−3	0.512934+/−10	+6.1	–	–	–	–
6606	0.70347+/−3	0.70346+/−3	0.512962+/−10	+6.6	18.718	15.578	38.558	–
6705	0.70334+/−3	0.70329+/−3	0.512990+/−10	+7.2	18.701	15.561	38.446	–
6707	0.70352+/−3	0.70352+/−3	0.513024+/−11	+7.9	18.728	15.577	38.549	–
6708	0.70317+/−3	–	0.513013+/−19	+7.7	18.551	15.544	38.319	–
6801	0.70317+/−3	0.70315+/−3	0.513018+/−10	+7.8	18.609	15.547	38.309	–
6803	0.70314+/−3	0.70315+/−3	0.513017+/−10	+7.8	18.672	15.558	38.384	–
1881-4	0.70317+/−3	0.70312+/−3	0.513006+/−10	+7.5	18.647	15.519	38.351	+5.3
1881-7	0.70312+/−3	0.70309+/−3	0.513013+/−10	+7.7	18.636	15.556	38.405	5.7

[a] Adjusted to E+A $SrCO_3$ $^{87}Sr/^{86}Sr = 0.70800$.
[b] Fractionation-corrected via NBS 981; external reproducibility +/− 0.05%/amu.

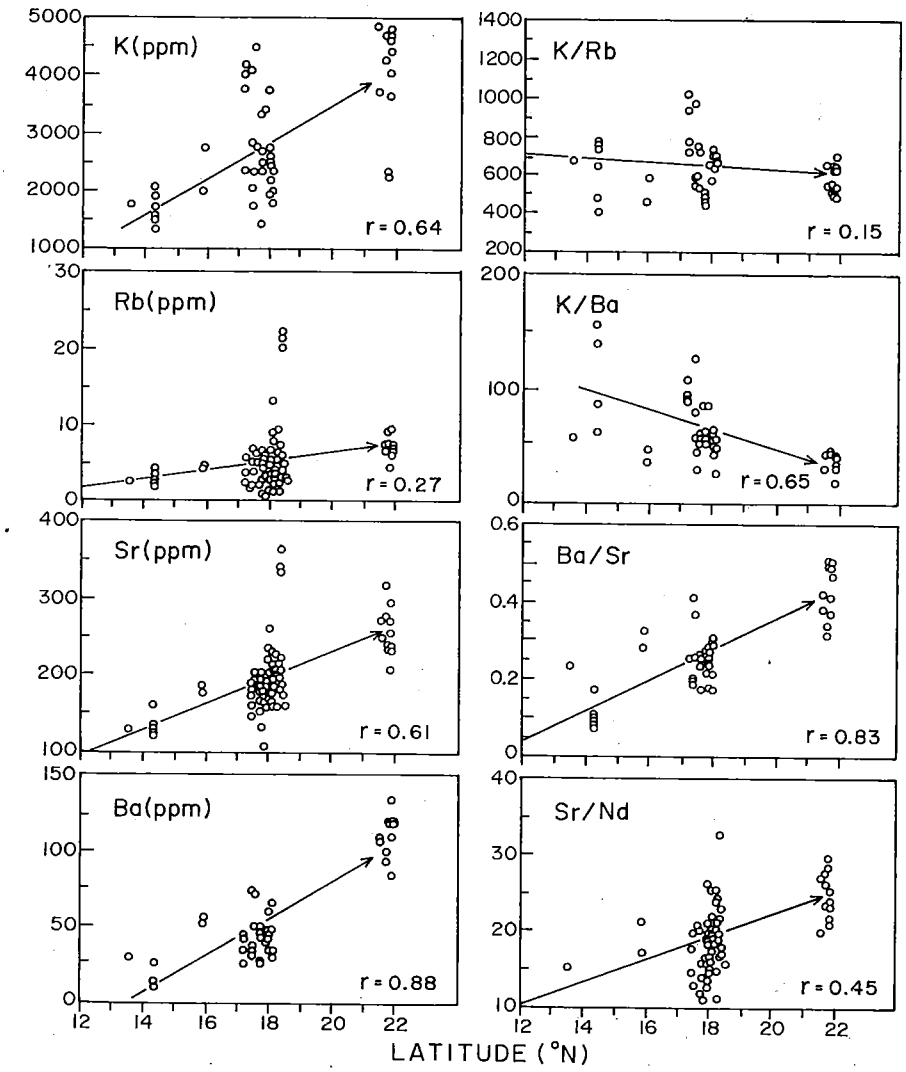

Fig. 3. Variation of incompatible elements K, Rb, Sr and Ba and incompatible element ratios K/Rb, K/Ba, Ba/Sr, and Sr/Nd as a function of latitude in the Mariana Trough. Correlation coefficients r are also given. MTB-22 data are from this study, other data from the literature [8,9,11–13].

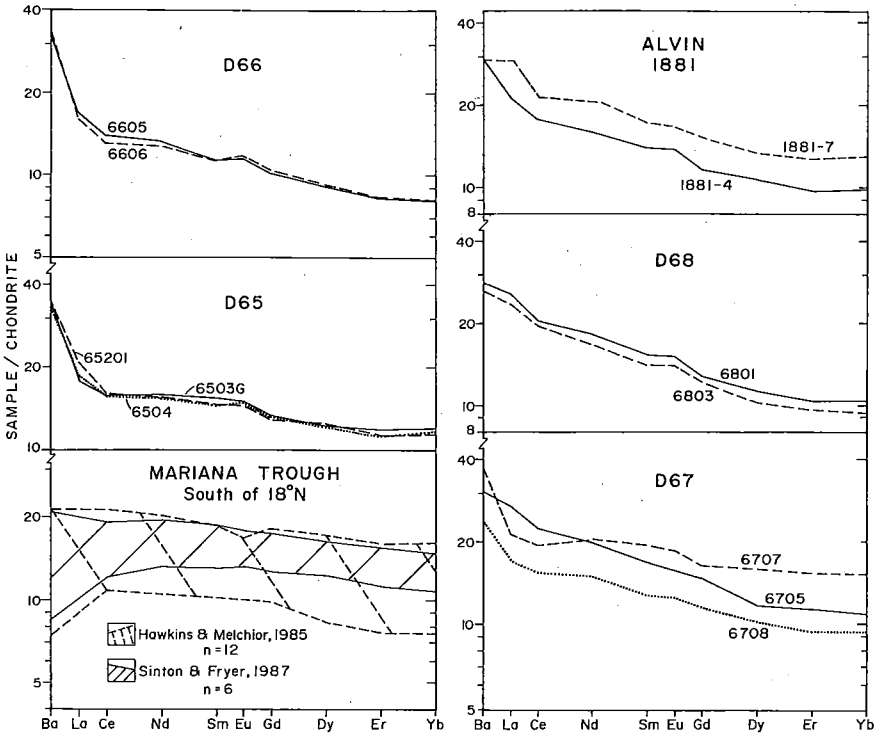

Fig. 4. Chondrite-normalized plots of Ba+REE for Mariana Trough basalts. In the lower left are plotted the fields outlined by REE patterns from 18° N and farther south [9,11]. The other portions of the diagram contain Ba+REE patterns for MTB-22, from this study.

the unusual "arc-like" samples of MTB-18 recovered from ALVIN dive 1846 are indistinguishable from MTB-22 [30]. The Nd isotopic composition of MTB-22 exhibits a modest range, with an epsilon-Nd between +8.1 and +6.1. This is generally lower than that for MTB-18 (excepting ALVIN 1846), characterized by epsilon-Nd in the range +9.3 to +11.9 (Fig. 6b), and is indistinguishable from Mariana arc CIP and S-NSP lavas (epsilon Nd = +6.4 to +8.1; [28,34,38–40]). A plot of Sr- vs. Nd- isotopic composition (Fig. 7) shows the transitional nature of the MTB-22 samples which plot between the fields defined for MTB-18 and Mariana arc lavas. Note that the high $^{87}Sr/^{86}Sr$ lavas, which plot clearly in the arc field, were unchanged by leaching.

The Pb isotopic compositions of MTB-22 are remarkably homogeneous, especially when compared with the large range of MTB-18 (Fig. 8a, b). The tight clustering of Pb-isotopic compositions is similar to that of the Mariana CIP, and the Pb-isotopic compositions of MTB-22 and CIP lavas are difficult to distinguish; the slightly higher delta-8/4 [41] of MTB-22 serves to best differentiate these two suites (Fig. 8a, b). MTB-22 have mean delta-7/4 of 4.2 ± 1.3 and delta-8/4 of 25 ± 5, normal values for mantle-derived melts from this part of the Pacific [41]. The range of $\delta^{18}O$ from MTB-22 glasses (+5.3 to +6.1) is very similar to that found for MTB-18 (+5.8 to +6.0) [42].

5. Discussion

The basalts from the Mariana Trough at 22° N have a clear arc signature, much stronger than those from farther south. In this discussion we first consider conditions and extent of melting. We then attempt to characterize the arc component and consider what this tells us about the evolution of the sources of back-arc and arc basalts and the location of these sources in the mantle.

5.1. Conditions of melting

The major element chemistry of MTB-22 is very similar to MTB-18, with the exception of slightly lower TiO_2 and slightly higher K_2O. Because both TiO_2 and K_2O behave as incompatible

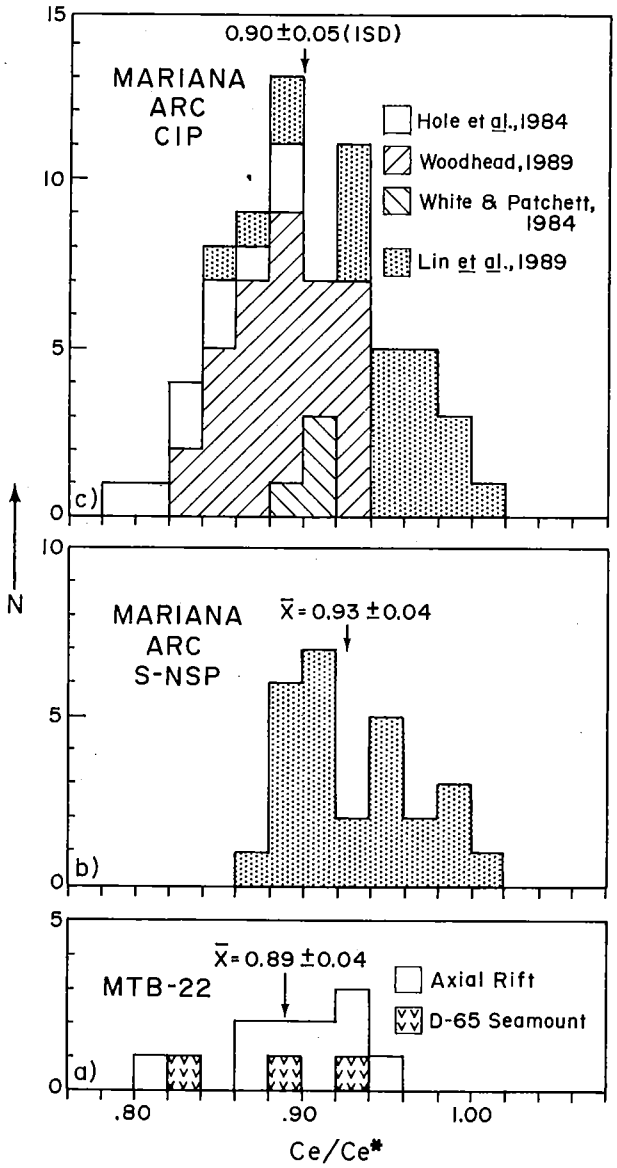

Fig. 5. Histograms of Ce/Ce* for MTB-22 and Mariana arc S-NSP and CIP [17,33,34,38]. Means with uncertainties are quoted at 1 std dev.

elements during melting and so should be enriched or depleted in tandem, this difference must reflect relatively minor differences in source compositions. This conclusion is strengthened by the systematic differences observed in trace elements (e.g., Ba/La and Sr/Nd). Furthermore, MTB-22 and MTB-18 fall on the global depth vs. Na_2O correlation [45] so that the inferences based on global MORB appear to apply to MTB. MTB-22 has $Na_{8.0} = 2.15 \pm 0.12$, significantly less than that for two MTB-18 sites listed in [45] ($Na_{8.0} = 2.63 \pm 0.04$, 2.77 ± 0.44). The analysis developed for

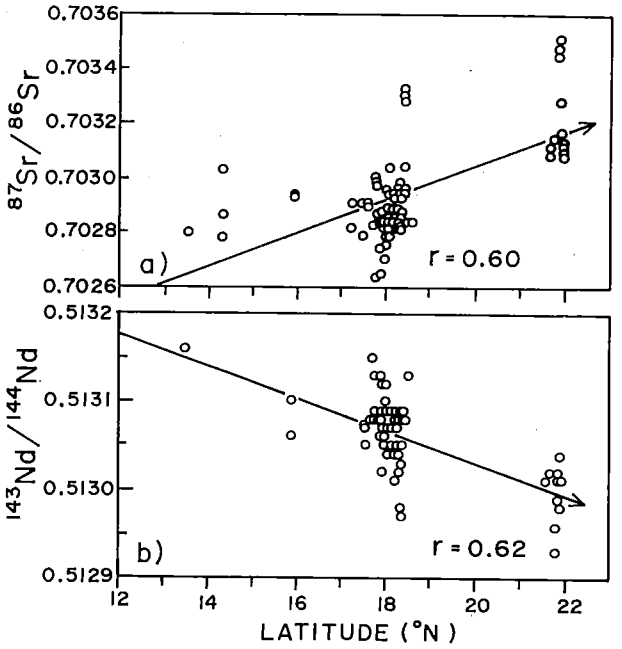

Fig. 6. Latitudinal variations in Sr isotopic compositions (a) and Nd isotopic compositions (b) in the Mariana Trough. Data sources are [8,9,13,30,37,42] and this study. Correlation coefficients r are also given.

global MORB indicates that MTB-22 represents a slightly higher degree of melting than that of MTB-18 ($F = 0.14$ vs. 0.11). To a first order, the

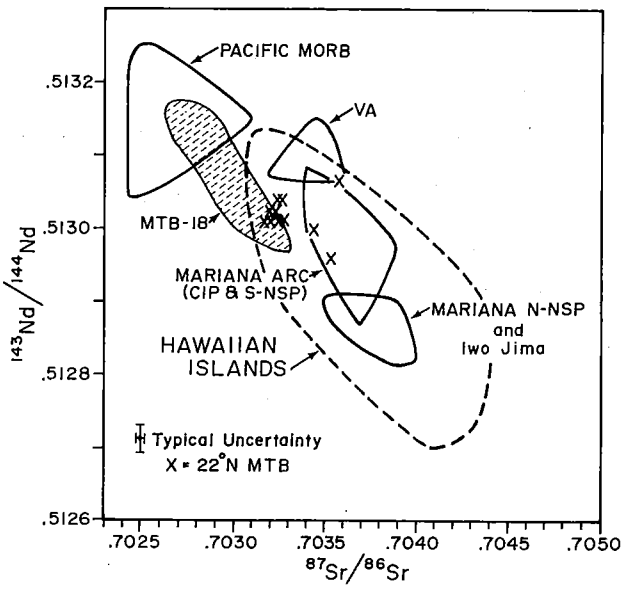

Fig. 7. Plot of Nd- vs. Sr- isotopic compositions for MTB-22. *VA* = Volcano arc, excluding Iwo Jima. Field labelled *Mariana Arc* includes data for Mariana CIP and S-NSP. Field labelled *N-NSP* is the northern part of the Northern Seamount Province and Iwo Jima. Data sources: 18° N MTB [13,30]; Mariana arc [28,34,38–40]; Mariana N-NSP and Iwo Jima [40]; references for Pacific MORB and Hawaii listed in [40].

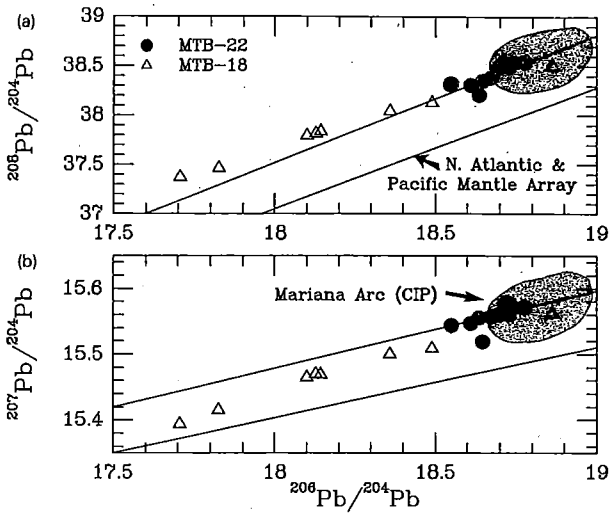

Fig. 8. Isotopic composition of Pb for MTB-22 (in dashed field) and other recent volcanics from the Mariana arc system; (a) plots $^{207}Pb/^{204}Pb$ vs. $^{206}Pb/^{204}Pb$; (b) plots $^{208}Pb/^{204}Pb$ vs. $^{206}Pb/^{204}Pb$. Data for 43 analyses for Mariana arc CIP are contained in the field outlined by a solid line and labelled *CIP* [35,55]. The six error bars that fall outside the MTB-22 field are MTB-18 [30]. The Northern Hemisphere Reference Line (NHRL) is also shown [41].

conclusions arrived at for the depth and percentage of melting of MTB-18 are applicable to MTB-22. MTB-18 is argued to have formed as a result of 15% melting of a pyrolitic mantle at pressures of between 5 and 15 kbar, or about 18 to 50 km depth [9,11]. This is in the range for the depth of generation of less than 65 km argued for Mariana arc melts on the basis of REE forward models [17].

5.2. Characterization of arc component in MTB-22

Both the Mariana arc and back-arc igneous systems show strong enrichments in LIL and LREE from 18° N northwards; these enrichments are accompanied by corresponding variation in radiogenic isotopic compositions. In the Mariana arc, these enrichments culminate in the shoshonitic rocks of the northern part of the Northern Seamount Province and Iwo Jima (N-NSP), typified by very high contents of LIL and LREE, with $(La/Yb)_n$ of 10–18, mantle-like Ba/La (15–20), radiogenic Sr (0.7035–0.7040) and non-radiogenic Nd (Epsilon-Nd = +2.4 to +5.0) [17,40]. These chemical and isotopic characteristics of the N-NSP contrast strongly with the chemical and isotopic features for the Mariana CIP and have been interpreted as reflecting increasing contribution from a more enriched, OIB-like mantle source. Eruption of shoshonitic lavas among volcanoes of the magmatic front in an intra-oceanic arc is unusual, interpreted to manifest unusual tectonic environments [43], and the shoshonitic association of the Mariana N-NSP and Iwo Jima has been interpreted to be a response to the northward propagation of the Mariana Trough back-arc extensional regime [14,44]. The point to be emphasized is that magma sources with strong enrichments in LIL and LREE elements exist beneath the northernmost Mariana arc, and, along with more normal Mariana arc sources—such as that of the CIP—may interact with the evolving MTB source.

It is thus important to know if the arc component apparent in MTB-22 is more like the N-NSP "shoshonitic" source (low Ba/La high $(La/Yb)_n$ Endmember II of [17]) or the less enriched arc sources of the CIP or S-NSP (high Ba/La, low $La/Yb)_n$ Endmember I of [17]). These possibilities can be scrutinized by plotting MTB-22 on a Ba/La vs. $(La/Yb)_n$ diagram developed for resolving the petrogenesis of arc melts (Fig. 9). Samples of MTB-22 plot between values typical of N-MORB and those of the source region for Mariana arc CIP and S-NSP lavas. The Nd–Sr isotopic data (Fig. 7) are best interpreted as resulting from mixing between mantle sources responsible for MORB and CIP-type melts, and the Pb isotopic data (Fig. 8) require a very large component of a CIP-type source. The fact that the MTB-22 data extends to a possible mixing curve between N-MORB and the shoshonitic Endmember II source is intriguing; sampling farther north is required to better evaluate whether or not the shoshonitic source is involved. We conclude from these data that, for the most part, the arc component in MTB-22 is that of typical, mature arcs such as the Mariana CIP or the geographically-associated S-NSP. Certainly the chemical and isotopic variations documented along the Mariana arc and the distinctions between this and other arc/back arc systems emphasizes the need to systematically compare back arc data with the associated volcanic arc.

5.3. Proportion of the arc component

The next question that needs to be answered is: "How much of the arc component is involved in

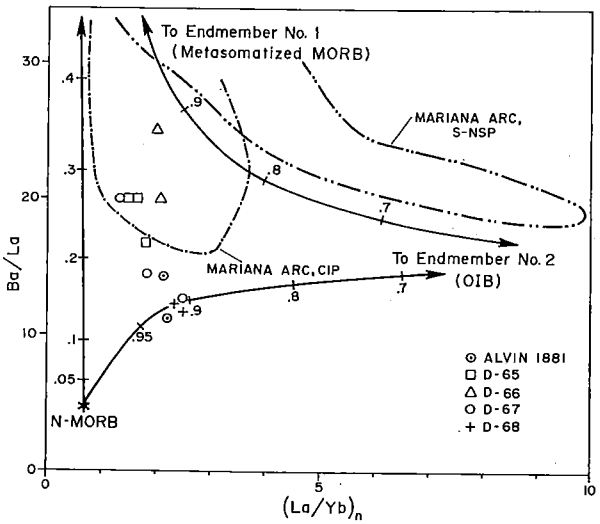

Fig. 9. Plot of Ba/La vs. $(La/Yb)_n$, showing the mixing trajectory calculated for Mariana arc lavas [17] and new trajectories for mixing between a MORB source and inferred Mariana arc sources. Tick marks on the mixing curves between Endmember #1 and MORB or Endmember #2 are the fraction of Endmember #1 (Metasomatized MORB-type mantle: high Ba/La; low La/Yb) involved in the mixture; tick marks between MORB and Endmember #2 are the fraction of MORB. Endmember #2 (OIB-type mantle: low Ba/La; high La/Yb) dominates source of the N-NSP shoshonites. Also shown is the field occupied by lavas from the Mariana arc CIP and S-NSP. Note that samples of MTB-22 lie between normal MORB and Endmember #1. Endmember #1 has Ba/La = 80 and $(La/Yb)_n = 0.5$. Endmember #2 has Ba/La = 15 and $(La/Yb)_n = 20$ [17]. MORB is modelled with Ba/La and La/Yb from [31]; all three endmembers are assumed to have equal Yb contents.

MTB-22 lavas?". This problem was examined for MTB-18, where a strong case for binary mixing of melts has been made [12,13,30]; these investigators argued that one endmember was MORB and the other was arc tholeiite. We note that the data do not allow one to distinguish between source mixing and melt mixing. This is because while Sr and Sm contents will be much greater in melts relative to sources, the Sm contents of these sources will be similar, as will be the case for their melts; also the Ba/Sm of arc melts and sources and MORB melts and sources will be similar [32]. Volpe et al. [13] developed a model in which MTB-18 melts result from 15–30% arc melt mixed with MORB melt; this model is equally appropriate for 15–30% source mixing. The same approach shows that MTB-22 reflect a much larger proportion, from 50 to 90%, of arc source or melt mixed with 10 to 50% MORB source or melt (Fig. 10). Basalts from the Mariana Trough north of 22°30′N (KK01, KK02; Fig. 1) have up to 1.04% K_2O and may manifest an even higher percentage of the arc component [16]—or the shoshonitic source.

As in all models, the calculated proportions are only approximations. The point labelled "Active Mariana arc" in Fig. 10 does not reflect the great variation in Mariana arc compositions. Regardless of the details of the model, MTB-22 are in many respects indistinguishable from Mariana arc lavas. Table 4 compares representative samples of MTB-22 with those from the adjacent portion of the Mariana arc. While there are subtle differences between the arc and back-arc samples (e.g., higher SiO_2, Al_2O_3 and $Fe_2O_3^T$, lower MgO in the arc), much of the variation may be attributed to increased fractionation of the arc lavas. If samples identical to MTB-22 were recovered from the arc, these would be well within the range of chemical and isotopic compositions expected for arc lavas, except that they are less fractionated. The point is that the chemical and isotopic compositions of MTB-22 are dominated by the arc component and the difficult problem is to identify the MORB component.

5.4. *Source mixing or metasomatism?*

The next problem to address is how the arc characteristics are imposed on the melt source of MTB-22. There are two end-member possibilities: (1) mixing between two chemically distinct mantle sources (or melts therefrom), one of which has strong arc chemical affinities; and (2) metasoma-

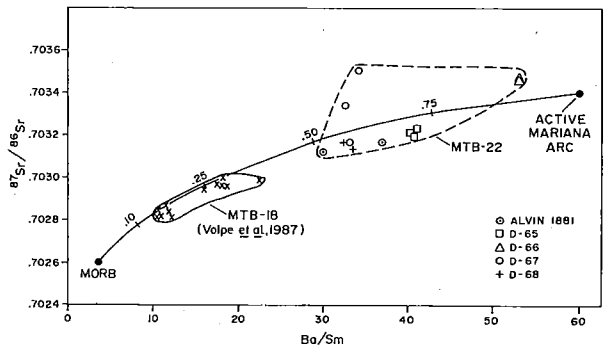

Fig. 10. Plot of $^{87}Sr/^{86}Sr$ vs. Ba/Sm and calculated mixing trajectory between MORB and basalt from the active Mariana arc, after [13]. Tick-marks on mixing trajectory indicate the proportion of the arc component in the mixture. Note that while MTB-18 requires 15–30% of the arc component, MTB-22 requires much more, 50–90% arc component.

TABLE 4
Comparison of arc and MTB-22 chemical and isotopic characteristics

	ARC		MTB-22	
	NW Uracas D19-3-10	Eifuku D31-2-2	D6605	1881-4
SiO_2	52.1	52.5	49.1	52.4
TiO_2	0.73	1.01	0.80	1.01
Al_2O_3	18.4	19.9	16.0	17.3
$Fe_2O_3^T$	10.6	11.3	8.53	8.52
MgO	5.60	3.72	10.1	6.50
Na_2O	2.12	2.83	2.04	2.86
K_2O	0.39	1.31	0.28	0.46
Rb(ppm)	7.3	25	4.5	6.5
Sr	265	706	238	272
Ba	155	448	120	104
La	2.54	21.4	5.51	6.99
Yb	1.85	1.90	1.78	2.18
Sr/Nd	52	33	28	27
Ba/La	61	21	20	14
K/Ba	23	24	19	34
$(La/Yb)_N$	0.92	7.5	2.1	2.1
K/Rb	496	422	498	552
$^{87}Sr/^{86}Sr$	0.70338	0.70348	0.70348	0.70312
ϵ_{Nd}	7.7 *	–	6.1 *	7.5 *

* From the northernmost part of the Mariana CIP and S-NSP [17,23,36].

tism, by subduction-related fluids, of a single, chemically homogeneous source. These possibilities are similar to those advanced to explain the evolution of the source of Mariana arc melts [17,33,34,40]. All investigators agree that a slab-derived component is needed to explain the high Ba/La, low $(La/Yb)_n$ source (Endmember I of [17]; Fig. 9); disagreement concerns whether or not mixing followed source metasomatism. In the case of the active Mariana arc, trace element and radiogenic isotopic data indicate that metasomatism of a MORB-like source produced a high Ba/La but LREE-depleted "Endmember I" which then mixed with low Ba/La, LREE-enriched "Endmember II" [17,40]. The observation that MTB-22 data plot between MORB (to the high La/Yb side) and extend towards "Endmember I" (Fig. 9) can be interpreted as resulting either from melting of a MORB source that was subjected to varying degrees of metasomatism by Ba-rich fluids or by melting of a mixture of MORB and "Endmember I" sources. The latter interpretation is similar to that proposed for MTB-18, which has an arc-like component ascribed to old oceanic lithosphere metasomatized by a previous subduction episode, with mixing between this and a MORB source being responsible for MTB-18 [30].

The models in Figs. 9 and 10 use the subduction-related (metasomatic?) enrichments of Ba to tag the arc source and monitor its mixing with MORB in the evolving BAB. This approach is sensitive to any subduction component but is insensitive to any differences between the arc and back-arc mantle that may relate to pre-existing mantle heterogeneity, previous melt extraction, variable residual mineralogies, etc. Consequently this approach must ultimately be combined with HFSE, compatible trace element, and REE diagrams to distinguish between the models sketched in Fig. 11. This approach has been used to evaluate the sources involved in generating Sumisu Rift basalts ands to conclude that differences between arc and back-arc include those related to and independent of subduction, and invoke mantle mixing as a primary mechanism [57].

For MTB-22, the predominance of the arc component is consistent with either the metasomatic or the mixing model. In the metasomatic model, the proximity of the rift to the arc places it's mantle source close to the origin of slab-derived metasomatic fluids, while for the mixing model, the arc component results from the arc source being intimately juxtaposed with the zone of mantle upwelling beneath the rift. For both models, the arc signature should diminish as the back-arc basin matures and widens, and the BAB source becomes increasingly separated from the subduction zone and the arc source.

Further sampling that shows the scale and regularity of the arc/back-arc transition with latitude may provide such insight. We expect that if the arc component has been imposed by metasomatism related to present subduction, there should be a gradual increase northward in this component, corresponding to the closer superposition of rift and subduction zone. If, however, the dominant process is mixing of older sources or melts, we expect that the trend of increasing arc component to the north may be more erratic, characterized by ridge segments erupting MTB-18 and MTB-22 in close proximity. We note that a small segment of the ridge at 18°N erupts basalts with chemical and isotopic compositions that are much more like MTB-22 than MTB-18 (ALVIN Dive 1846). These

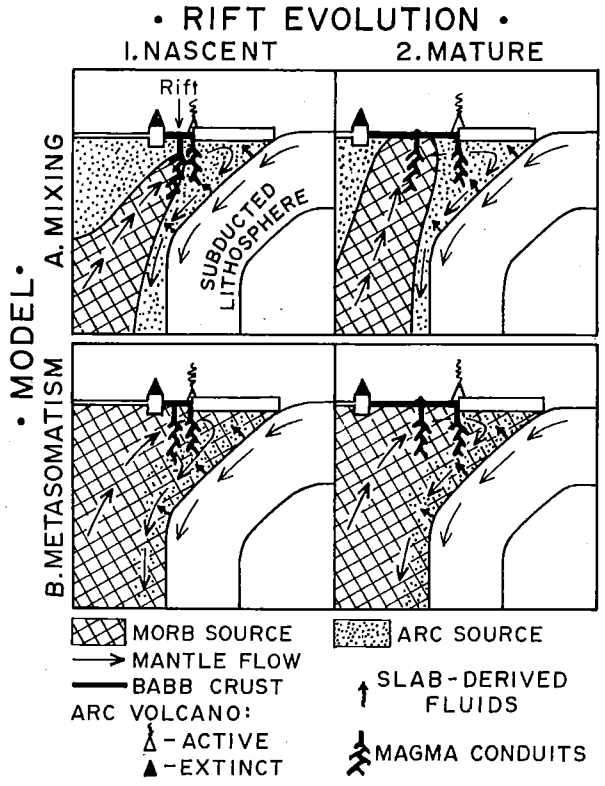

Fig. 11. Tectonic cartoons showing the two endmember models which can explain the arc-like composition of basalts erupted in juvenile BAB such as the Marianas and how the composition of BAB magmas evolves towards MORB as such rifts mature. (A) The model of mixing between MORB-like and arc-like mantle sources is shown in the top two panels. (1) The nascent rift is accompanied by upwelling of MORB-like mantle which, because of the proximity of the arc and the rift, mixes with the arc source that it displaces. (2) As the rift widens, the progressive separation of the MORB and arc sources restricts their interaction. (B) The model of metasomatism of a MORB-like source is shown on the lower two panels. (1) Because of its proximity to the arc, the nascent rift begins over the subduction zone, where a MORB-like mantle source is metasomatized by hydrous fluids derived from the subducting lithosphere. (2) As the rift widens, the site of magma generation becomes isolated from the effects of subduction-related fluids.

are found along a ridge segment that predominantly produces typical MORB-like MTB-18. This scale of heterogeneity is much more consistent with a model of source- or melt-mixing than it is with one of metasomatism. For this reason we prefer the model of source- or melt-mixing over one of variable metasomatism as being the most important control of MTB-22 compositions.

5.5. Implications for the magmatic evolution of back-arc basins

The preceding data and interpretations lead us to conclude that the young Mariana Trough erupted basalts with strong arc affinities. In this section we examine whether or not this is a general result, based on geochemical and isotopic studies of other BAB.

There are several other BAB systems that show a strong arc signature in their early evolutionary stages. Hawkins and Melchior [9] argued that the northern Lau Basin shows a compositionally zoned crust, with a decrease in the proportion of the arc component observed with widening of the basin. The crust that formed just after arc rifting has strong arc affinities compared to that which formed later, as the BAB widened and matured. The identification of remarkably arc-like lavas from the Valu Fa ridge in the southern Lau Basin [46], where the active axis of the BAB is immediately adjacent to the arc, strengthens their argument. A corresponding zonation of the Mariana Trough has not been identified, but this may be due to inadequate sampling of the early BAB crust. The data for MTB-22 does indicate, however, that the narrow parts of the Mariana Trough are dominated by arc-like basalts, and leads us to predict that when better sampling of the older crust in the Trough is accomplished, it will show a strong arc chemical signature.

The Bransfield Strait, Antarctica, is interpreted as the site of a very early stage BAB [47]. Basalts erupted from three islands in this rift have incompatible element concentrations that are intermediate between arc tholeiites and calc-alkaline lavas. The Bransfield Strait lavas are significantly enriched in Ba in particular and depleted in HFSC such as Ti, Zr, Nb, and Y. These characteristics are interpreted as typical of island arc tholeiite suites and ascribed [47] to the "...complex nature of the mantle under an active island arc combined with complex melting relationships attending the initial stages of back-arc spreading".

Rifting of the New Hebrides arc has formed the Coriolis Trough and the Northern Basin, interpreted as initial stage rifts in the development of a back-arc basin [48]. Futuna Island, a volcano that formed during intial rifting, is composed of basalts and basaltic andesites that have all the petrographic and geochemical characteristics of arc

lavas. This igneous succession was interpreted as indicating that the earliest stages in back-arc evolution result in the eruption of arc-like magmas [49].

The Sumisu Rift (SR) is an excellent example of the early stages in the evolution of BAB [50]. SR basalts have major element compositions indistinguishable from basalts erupted from mature BAB [50–52]. The trace elements for SR basalts show only a slight arc signature; in particular, the enrichments in Ba found for MTB-22 are not observed [50–52]. If correct, this interpretation means that the model constructed for the Mariana Trough is not globally applicable. This is the Sumisu Rift–Mariana Trough paradox: Sumisu Rift lavas erupted 20–40 km behind the Izu volcanic front show only a small arc imprint whereas MTB-22 basalts, erupted 50–100 km behind the volcanic front, show a very large one.

The reasons behind the apparent paradox may be both complex and important. The transition from arc to back-arc is also the transition from a more to a less hydrous melting environment and so also involves different degrees or conditions of melting and different residual mineralogies and/or fractionating assemblages [50–52,57]. The diminishing volatile content of the back-arc presumably accompanies a diminishing subduction signature in trace element and isotopic characteristics. These effects will be superimposed on those deriving from the pre-existing chemistry of the sub-arc mantle and any new material introduced to the region through rifting as well as the mixing between them. Different elements will respond to different aspects of the transition: major elements will be most sensitive to conditions of melting and to fractionating assemblages. LIL elements (Cs, Rb, Ba) will reflect the hydrous metasomatic component, both old and new. In contrast, HFSE and REE may reflect prior melting history and composition of the sub-arc mantle as well as mixing proportions.

The contrasts between MTB-22 and SR basalts raise the possibility that the transition from arc to back-arc may not be spatially or temporally identical in different regions. In this context, the chemistry of Izu and Mariana arc "cross-chain seamounts" is noteworthy [50,53]. These cross-chains are part of the active arc but erupt lavas that are distinct from the more voluminous magmas erupted along the volcanic front in having stronger enrichments in LREE and less relative enrichments in Ba [16,50]. The Kasuga seamounts in the Mariana arc are the best studied cross-chain; geochemical and isotopic studies suggest that these lavas are derived from a mantle source that is very different from that responsible for lavas erupted along the magmatic front of the CIP and S-NSP (i.e., insignificant proportion of "Endmember I" [17]). The mantle source responsible for both SR and Mariana arc cross-chains has characteristics that may be appropriate to be involved in the generation of SR basalts (i.e., LREE enrichment, low Ba/REE).

6. Conclusions

Basalts erupted near the northern terminus of the Mariana Trough bear strong chemical and isotopic similarities to the composition of Mariana arc lavas, in particular to those erupted at similar latitude along the arc. We propose that this arc component may become involved either by mixing of arc and MORB mantle sources or by variable metasomatism of a MORB-like mantle by subduction-related metasomatic fluids. The evolution of basalt compositions in the Mariana Trough reflects the progressively greater role of the MORB source, either as a result of physical isolation of the arc source from the zone of mantle upwelling beneath the rift or by the progressive separation of this zone from the site of subduction-related metasomatism (Fig. 11). This model is consistent with magmatic evolution inferred from several other incipient and mature back-arc basin systems, with the possible exception of the Sumisu Rift. Consideration of more heterogeneous arc sources may reconcile this paradox.

Acknowledgements

The samples analyzed here were collected in the course of expeditions funded by the U.S. National Science Foundation. Analytical work was supported under NSF grants OCE-8812442 to Stern, OCE-8410596 to Fryer, and OCE-8515887 to Ito. We are grateful to Terry Plank for an incisive and constructive review. This is UTD Programs in Geosciences Contribution No. 654.

Appendix 1—petrographic descriptions

65201: Vesicular, sparsely phyric basalt (~ 2% microphenocrysts of CPX and PLAG, ~ 20% irregular vesicles). Glass is devitrified. *6503*: Sparsely phyric basalt (~ 2% phenocrysts and microphenocrysts of CPX and PLAG). *6504*: Sparsely phyric basalt (~ 2% phenocrysts and microphenocrysts of CPX and PLAG). *6605*: Porphyritic basalt (~ 9% OL and ~ 10% PLAG phenocrysts and microphenocrysts), occasionally glomerophyric. ~ 10% small vesicles; abundant glass. *6606*: Porphyritic basalt (~ 15% OL and ~ 10% PLAG phenocrysts and microphenocrysts; minor CPX megacrysts), occasionally glomerophyric. ~ 10% small vesicles; some glass. *6705*: Aphyric basalt, with PLAG and CPX microphenocrysts; ~ 20% vesicles. *6707*: Aphyric basalt; rare PLAG and CPX microphenocrysts; ~ 15% vesicles. *6708*: Porphyritic basalt (10% OL, ~ 3% CPX, ~ 5% PLAG). Moderately vesicular; abundant glass. *6801*: Porphyritic basalt (~ 5% OL, ~ 10% PLAG), ~ 30% vesicles. *6803*: Porphyritic basalt (~ 10% OL, ~ 5% PLAG), > 30% vesicles, abundant glass. *1881-4*: Sparsely phyric basalt (~ 5% OL and ~ 10% PLAG microphenocrysts), ~ 15% vesicles. Abundant fresh glass on margins. *1881-7*: Sparsely phyric basalt (~ 10% PLAG, ~ 3% OL, ~ 1% CPX microphenocrysts) ~ 20% vesicles. Hyalopilitic groundmass with abundant glass.

References

1 D.E. Karig, Origin and development of marginal basins in the western Pacific, J. Geophys. Res. 76, 2452–2561, 1971.
2 J.W. Hawkins, S.H. Bloomer, C.A. Evans, and J.T. Melchior, Evolution of intra-oceanic arc-trench systems. Tectonophysics 102, 175–205, 1984.
3 D.E. Karig, Structural history of the Mariana Island arc system, Geol. Soc. Am. Bull. 82, 323–344, 1971.
4 D.M. Hussong, S. Uyeda et al., eds., Initial Reports of the Deep Sea Drilling Project 60, U.S. Gov. Printing Off., 929 pp., Washington, D.C., 1981.
5 L.D. Bibee, G.G. Shor, Jr. and R.S. Lu, Inter-arc spreading in the Mariana Trough, Mar. Geol. 35, 183–197, 1980.
6 T. Eguchi, Seismotectonics around the Mariana Trough, Tectonophysics 102, 33–52, 1984.
7 P. Lonsdale and J. Hawkins, Silicic volcanism at an off-axis geothermal field in the Mariana Trough back-arc basin, Geol. Soc. Am. Bull. 96, 940–951, 1985.
8 S.R. Hart, W.E. Glassley and D.E. Karig, Basalts and sea-floor spreading behind the Mariana Island arc, Earth Planet. Sci. Lett. 15, 12–18, 1972.
9 J.W. Hawkins and J.T. Melchior, Petrology of Mariana Trough and Lau Basin basalts, J. Geophys. Res. 90, 11, 431–11, 468, 1985.
10 R. Poreda, Helium-3 and deuterium in back-arc basalts: Lau Basin and the Mariana Trough, Earth Planet. Sci. Lett. 73, 244–254, 1985.
11 J.H. Sinton and P. Fryer, Mariana Trough lavas from 18° N: Implications for the origin of back arc basin basalts, J. Geophys. Res. 92, 12, 782–12, 802, 1987.
12 D.A. Wood, N.G. Marsh, J. Tarney, J.-L. Joron, P. Fryer and M. Treuil, Geochemistry of igneous rocks recovered from a transect across the Mariana Trough, arc, fore-arc, and trench, Sites 453 through 461, Deep Sea Drilling Project Leg 60, in: D.M. Hussong, S. Uyeda, et al., eds., Init. Rep. DSDP 60, Gov. Print. Off., Washington, D.C., pp. 611–645, 1981.
13 A.M. Volpe, J.D. Macdougall and J.W. Hawkins, Mariana Trough basalts (MTB): Trace element and Sr–Nd isotopic evidence for mixing between MORB-like and arc-like melts, Earth Planet. Sci. Lett. 82, 241–254, 1987.
14 R.J. Stern, N.C. Smoot and M. Rubin, Unzipping of the Volcano arc, Japan, Tectonophysics, 102, 153–174, 1984.
15 A.T. Hsui and S. Youngquist, A dynamic model of the curvature of the Mariana Trench, Nature 318, 455–457, 1985.
16 M.C. Jackson, Petrology and petrogenesis of recent submarine volcanics from the northern Mariana arc and back-arc basin, Ph.D. Dissertation, Univ. Hawaii, 277 pp., 1989.
17 P.-N. Lin, R.J. Stern and S.H. Bloomer, Shoshonitic volcanism in the northern Mariana arc. 2. Large-ion lithophile and rare earth element abundances: evidence for the source of incompatible element enrichments in intraoceanic arcs, J. Geophys. Res. 94, 4497–4514, 1989.
18 P. Richard, N. Shimizu and C.J. Allègre, $^{143}Nd/^{146}Nd$, a natural tracer. An application to oceanic basalts, Earth Planet. Sci. Lett. 31, 269–278, 1976.
19 R.J. Walker, R.W. Carlson, S.B. Shirey and F.R. Boyd, Os, Sr, Nd and Pb isotope systematics of southern African peridotite xenoliths: Implications for the chemical evolution of the subcontinental mantle, Geochim. Cosmochim. Acta 53, 1583–1596, 1989.
20 J. Borthwick and R.S. Harmon, A note regarding ClF_3 as an alternative to BrF_5 for silicate oxygen isotope analysis. Geochim. Cosmochim. Acta 46, 1665–1669, 1982.
21 R.N. Clayton and T.K. Mayeda, The use of bromine pentafluoride in the extraction of oxygen from oxides and silicates for isotopic analysis. Geochim. Cosmochim. Acta 27, 43–52, 1963.
22 R.J. Stern, On the origin of andesite in the northern Mariana Island arc: Implications from Agrigan, Contrib. Mineral. Petrol. 86, 207–219, 1979.
23 T.H. Dixon and R. Batiza, Petrology and chemistry of Recent volcanics in the Northern Marianas: Implications for the origin of island arc basalts, Contrib. Mineral. Petrol. 70, 167–181, 1979.
24 A. Meijer and M. Reagan, Petrology and geochemistry of the island of Sarigan in the Mariana Arc: Calc-alkaline volcanism in an oceanic setting, Contrib. Mineral. Petrol. 77, 337–354, 1981.
25 S.H. Bloomer, R.J. Stern, E. Fisk and C.H. Geschwind,

Shoshonitic volcanism in the northern Mariana arc 1. Mineralogic and major and trace element characteristics, J. Geophys. Res. 94, 4469–4496, 1989.
26 A.Y. Sharaskin, Petrography and geochemistry of basement rocks from five Leg 60 sites, in: D.M. Hussong, S. Uyeda, et al., eds., Init. Rep. DSDP 60, Gov. Print. Off., Washington, D.C., pp. 647–656, 1981.
27 E.E. Larson, R.L. Reynolds, R. Merrill, S. Levi, M. Ozima, Y. Aoki, H. Kinoshita, S. Zasshu, N. Kawai, T. Nakamura and K. Hirooka, Major element petrochemistry of some extrusive rocks from the volcanically active Marianas Islands, Bull. Volcanol. 38, 361–377, 1974.
28 R.J. Stern and L.D. Bibee, Esmeralda Bank: Geochemistry of an active submarine volcano in the Mariana Island arc, Contrib. Mineral. Petrol. 86, 159–169, 1984.
29 T.H. Dixon and R.J. Stern, Petrology, chemistry and isotopic composition of submarine volcanoes in the southern Mariana arc, Geol. Soc. Am. Bull. 94, 1159–1172, 1983.
30 A.M. Volpe, J.D. Macdougal, G.W. Lugmair, J.W. Hawkins and P. Lonsdale, Fine-scale isotopic variation in Mariana Trough Basalts: evidence for heterogeneity and a recycled component in backarc basin mantle, Earth Planet. Sci. Lett. 100, 251–264 (this volume).
31 A.W. Hofmann, Chemical differentiation of the Earth: the relationship between mantle, continental crust and oceanic crust, Earth Planet. Sci. Lett. 90, 297–314, 1988.
32 M.R. Perfit, D.A. Gust, A.E. Bence, R.J. Arculus and S.R. Taylor, Chemical characteristics of island-arc basalts: implications for mantle sources, Chem. Geol. 30, 227–256, 1980.
33 M.J. Hole, A.D. Saunders, G.F. Marriner and J. Tarney, Subduction of pelagic sediments: Implications for the origin of Ce-anomalous basalts from the Mariana Islands, J. Geol. Soc. London 141, 453–472, 1984.
34 J.D. Woodhead, Geochemistry of the Mariana arc (western Pacific): Source composition and processes, Chem. Geol. 76, 1–24, 1989.
35 A. Meijer, Pb and Sr isotopic data bearing on the origin of volcanic rocks from the Mariana island-arc system, Geol. Soc. Am. Bull. 87, 1358–1369, 1976.
36 H.E. Newsom, W.M. White, K.P. Jochum and A.W. Hofmann, Siderophile and chalcophile element abundances in oceanic basalts, Pb isotope evolution and growth of the earth's core, Earth Planet. Sci. Lett. 80, 299–313, 1986.
37 R.J. Stern, Strontium isotopes from circum-Pacific intraoceanic island arcs and marginal basins: Regional variations and implications for magmagenesis, Geol. Soc. Am. Bull. 93, 477–486, 1982.
38 W.M. White and J. Patchett, Hf–Nd–Sr isotopes and incompatible element abundances in island arcs: Implications for magma origins and crust–mantle evolution, Earth Planet. Sci. Lett. 67, 167–185, 1984.
39 D.J. DePaolo and G.J. Wasserburg, The sources of island arcs as indicated by Nd and Sr isotopic studies, Geophys. Res. Lett. 4, 465–468, 1977.
40 P.-N. Lin, R.J. Stern, J. Morris and S.H. Bloomer, Nd- and Sr- isotopic composition of lavas from the northern Mariana and southern Volcano arcs: Implications for the origin of island arc melts, Contrib. Mineral. Petrol., in press.
41 S.R. Hart, A large-scale isotope anomaly in the Southern Hemisphere mantle, Nature 309, 753–757, 1984.
42 E. Ito and R.J. Stern, Oxygen- and strontium-isotopic investigations of subduction zone volcanism: The case of the Volcano arc and the Mariana Island arc, Earth Planet. Sci. Lett 76, 312–320, 1986.
43 S.E. DeLong, F.N. Hodges and R.J. Arculus, Ultramafic and mafic inclusions, Kanaga Island, Alaska and the occurrence of alkaline rocks in island arcs, J. Geol. 83, 721–736, 1975.
44 R.J. Stern, P.-N. Lin, S.H. Bloomer, E. Ito and J. Morris, LIL- and LREE- enriched magmatism in Mariana Arc Seamounts: Effect of propagating back-arc extension, Geology 16, 426–430, 1988.
45 E.M. Klein and C.H. Langmuir, Global correlations of ocean ridge basalt chemistry with axial depth and crustal thickness. J. Geophys. Res. 92, 8089–8115, 1987.
46 G.A. Jenner, P.A. Cawoud, M. Rautenschlein and W.M. White, Composition of back-arc basin volcanics, Valu Fa Ridge, Lau basin: Evidence for a slab-derived component in their mantle source, J. Volcanol. Geotherm. Res. 32, 209–222, 1987.
47 S.D. Weaver, A.D. Saunders, R.J. Pankhurst and J. Tarney, A geochemical study of magmatism associated with the initial stages of back-arc spreading. Contrib. Mineral. Petrol. 68, 151–169, 1979.
48 J. Dubois, F. Dugas, A. Lapouille and R. Louat, The troughs at the rear of the New Hebrides island arc: Possible mode of formation, Can. J. Earth Sci. 15, 351–360, 1978.
49 G. Marcelot, C. Dupuy, M. Girod and R.C. Maury, Petrology of Futuna Island lavas (New Hebrides): An example of calc-alkaline magmatism associated with the initial stages of back-arc spreading Chem. Geol. 38, 23–37, 1983.
50 Y. Ikeda and M. Yuasa, Volcanism in nascent back-arc basins behind the Shichito Ridge and adjacent areas in the Izu–Ogasawara arc, northwest Pacific: Evidence for mixing between E-type MORB and island arc magmas at the initiation of back-arc rifting, Contrib. Mineral. Petrol. 101, 377–393, 1989.
51 P. Fryer, B. Taylor, C.H. Langmuir and A.G. Hochstaedter, Petrology and geochemistry of lavas from the Sumisu and Torishima backarc rifts, Earth Planet. Sci. Lett. 100, 161–178 (this volume).
52 A.G. Hochstaedter, J.B. Gill, M. Kusakabe, S. Newman, M. Pringle, B. Taylor and P. Fryer, Volcanism in the Sumisu Rift, I. Major element, volatiles and stable isotope chemistry, Earth Planet. Sci. Lett. 100, 179–194 (this volume).
53 D.M. Hussong and P. Fryer, Back-arc seamounts and the SeaMARC II seafloor mapping system, EOS 64, 627–632, 1983.
54 P. Fryer, J.M. Sinton and J.A. Philpotts, Basaltic glasses from the Mariana Trough, in: D.M. Hussong, S. Uyeda, et al., eds., Init. Rep. DSDP 60, Gov. Print. Off., Washington, D.C., pp. 601–609, 1981.
55 J.D. Woodhead and D.G. Fraser, Pb, Sr and ^{10}Be isotopic studies of volcanic rocks from the Northern Mariana Islands: Implications for magma genesis and crustal recycling in the Western Pacific, Geochim. Cosmochim. Acta 49, 1925–1930, 1985.
56 T.N. Irvine and W.R.A. Baragar, A guide to the chemical classification of the common volcanic rocks, Can. J. Earth Sci. 8, 523–548, 1971.
57 A.G. Hochstaedter, J.B. Gill and J.D. Morris, Volcanism in the Sumisu Rift, II. Subduction and non-subduction related components, Earth Planet. Sci. Lett. 100, 195–209 (this volume).